Engineering 7 (2021) 153–161

Contents lists available at ScienceDirect

Engineering

journal homepage: www.elsevier.com/locate/eng

Research
Tissue Engineering—Article

Enhancing the Surface Properties of a Bioengineered Anterior Cruciate Ligament Matrix for Use with Point-of-Care Stem Cell Therapy

Xiaohua Yu [a,b,c,#], Paulos Y. Mengsteab [a,b,c,d,#], Ganesh Narayanan [a,b,c], Lakshmi S. Nair [a,b,c,d,e], Cato T. Laurencin [a,b,c,d,e,f,g,*]

[a] Connecticut Convergence Institute for Translation in Regenerative Engineering, University of Connecticut Health, Farmington, CT 06030, USA
[b] Raymond and Beverly Sackler Center for Biological, Physical and Engineering Sciences, University of Connecticut Health, Farmington, CT 06030, USA
[c] Department of Orthopedic Surgery, University of Connecticut Health, Farmington, CT 06030, USA
[d] Department of Biomedical Engineering, University of Connecticut, Storrs, CT 06269, USA
[e] Department of Materials Science and Engineering, University of Connecticut, Storrs, CT 06269, USA
[f] Department of Chemical and Biomolecular Engineering, University of Connecticut, Storrs, CT 06269, USA
[g] Department of Reconstructive Sciences, University of Connecticut Health, Farmington, CT 06030, USA

ARTICLE INFO

Article history:
Received 8 August 2019
Revised 26 December 2019
Accepted 3 February 2020
Available online 7 May 2020

Keywords:
Anterior cruciate ligament
Ligament
Poly(*L*-lactic) acid plasma treatment
Fibronectin
Stem cells
Adhesion

ABSTRACT

We have previously developed a poly(*L*-lactic) acid (PLLA) bioengineered anterior cruciate ligament (ACL) matrix that has demonstrated enhanced healing when seeded with primary ACL cells prior to implantation in a rabbit model, as compared with the matrix alone. This suggests that improving cell adhesion on the matrix may beneficially affect the healing response and long-term performance of the bioengineered ACL matrix. One regenerative engineering approach involves enhancing the surface properties of the matrix to support cell adhesion and growth in combination with point-of-care stem cell therapy. Herein, we studied the cell adhesion properties of PLLA braided microfiber matrices enhanced through the physical adsorption of fibronectin and air plasma treatment. We evaluated the kinetics and binding efficiency of fibronectin onto matrices at three time points and three fibronectin concentrations. Incubating the matrix for 120 min in a solution of 25 $\mu g \cdot mL^{-1}$ fibronectin achieved the greatest binding efficiency to the matrix and cellular adhesion. Exposing the matrices to air plasma treatment for 5 min before fibronectin adsorption significantly enhanced the cell adhesion of rabbit bone marrow-derived mesenchymal stem cells (R-BMMSCs) 24 h post cell seeding. Finally, cellular proliferation was monitored for up to 21 d, the matrices were exposed to air plasma treatment, and fibronectin adsorption was found to result in enhanced cell number. These findings suggest that exposure to air plasma treatment and fibronectin adsorption enhances the cellular adhesion of PLLA braided microfiber matrices and may improve the clinical efficacy of the matrix in combination with point-of-care stem cell therapies.

1. Introduction

The anterior cruciate ligament (ACL) is the most commonly injured ligament of the human knee. Ligament injuries heal slowly and poorly because of limited vascularization, and therefore require surgical intervention. With more than 2.5×10^5 ACL reconstruction surgeries being performed in the United States per year, the annual cost to the healthcare system is approximately 18 billion USD [1]. Current treatments involve either the use of patients' own patellar or hamstring tendons (autografts) or allografts [2–4]. The limitations associated with the use of autografts include limited availability and potential donor site morbidity. Allografts can potentially transmit disease and may elicit an unfavorable immunogenic response from the host. Synthetic non-degradable replacements based on carbon fibers, polyethylene terephthalate (Leeds-Keio ligament), polypropylene (Kennedy ligament augmentation device), and polytetrafluoroethylene (Gore-Tex®) have shown limited success and suffer from stress shielding, fatigue, creep, and wear debris, which can eventually lead to osteoarthritis and synovitis [5–11]. These synthetic replacements act as

* Corresponding author.
E-mail address: laurencin@uchc.edu (C.T. Laurencin).
# These authors contributed equally to this work.

https://doi.org/10.1016/j.eng.2020.02.010

prosthetics and are not designed to regenerate native ACL tissue. Consequently, there is a pressing need to develop an alternative treatment strategy that results in the regeneration of ligamentous tissues. Our preliminary *in vitro* and small animal studies have demonstrated the feasibility of developing a bioengineered and biodegradable three-dimensional (3D) scaffold that can support ligament regeneration [12,13]

We first investigated the suitability of different synthetic polymeric fibers for developing the 3D construct [14]. Of the different biodegradable and biocompatible synthetic polymers investigated, poly(*L*-lactic acid) (PLLA) fibers were selected based on their structural integrity and superior mechanical properties over time, as well as the US Food and Drug Administration (FDA) clearance status of this polymer for a variety of clinical applications [15]. The 3D structure of the scaffold plays an essential role in cellular ingrowth and tissue regeneration, and requires constructs with controlled pore size, integrated pores, and mechanical properties comparable to those of the natural ACL [16]. Therefore, we developed a braided scaffold with a hierarchical structure like the natural ACL composed of PLLA microfibers that are arranged in bundles and wound throughout the thickness of the scaffold. The hierarchical structure was created using braids with three regions: a femoral tunnel attachment site, an intra-articular zone, and a tibial tunnel attachment site [17]. The fiber orientation was varied to induce changes in pore sizes in order to encourage ligament and bone ingrowth and promote vascularization in these different regions. The pore sizes were approximately in the range of 150 μm for the bony attachment area and 200–250 μm for the intra-articular region, based on studies indicating optimal pore size for bone and soft tissue ingrowth [18]. In addition, the braiding process developed a continuous interconnected pore structure and increased the available surface area for cell attachment, which could lead to an enhanced regenerative response by allowing tissue ingrowth throughout the matrix [16]. Our *in vitro* studies supported the hypothesis by showing the ability of the structure to support cell adhesion, growth, and matrix deposition [19]. From a biomechanical perspective, the relatively lower pore size or higher braiding angle at the bony attachment sites might significantly improve the quality of anchorage in bone tunnels and provide resistance to wear. Moreover, the unique braiding process permitted fibers to be woven throughout the entire thickness of the braid, allowing for increased braid toughness and reinforcement to prevent rupture [14]. The initial proof of concept of the design was tested in a rabbit model, and that study demonstrated the feasibility of implanting the 3D scaffold and the ability of the structure to support tissue ingrowth [12]. Through the 12 week implantation study, we also demonstrated that the combination of a scaffold with primary ACL cells yielded better results than those of a polymer replacement without cell seeding [12]. It is thus expected that cell seeding can beneficially affect the healing response and long-term performance of bioengineered ACL replacements.

Advances in regenerative engineering have yielded significant insights into the importance of the surface properties of the natural extracellular matrix (ECM) (e.g., surface energy, morphology, and ECM components) on cell behavior and consequent tissue formation [20]. For example, the effect of material surface energies on cell adhesion has been well documented in the literature: High hydrophobicity (a water drop contact angle of approximately 100° or more) is believed to be disadvantageous to cell adhesion, while highly hydrophilic surfaces are not conducive to the adsorption of proteins [21]. Hanson et al. [22] demonstrated that enhanced adhesion of mesenchymal stem cells (MSCs) on PLLA scaffolds could be achieved using oxygen plasma treatment. It is also known that specific ECM subunits interact with integrins and other cell surface receptors, leading to specific cell responses that include adhesion, proliferation, and differentiation [23]. Coating ECM components on scaffold surfaces creates biological cues that exerts a beneficial effect on cellular response and tissue repair. The advantages of this method are as follows: ① These proteins/glycoproteins are easily and inexpensively extracted from natural sources; ② the coating of ECM components on the surface can be easily achieved by various mild coating/deposition methods; and ③ the retention and release of ECM components can be efficiently regulated by tuning the material surface chemistry. Several ECM components, including type I collagen and fibronectin, have been found to be biologically active in ligament development and regeneration [24–29]. For example, cellular proliferation and tissue growth on the scaffold have been enhanced by the presence of fibronectin [14,18,30,31]. In addition to being one of the most abundant extracellular glycoproteins found in the body, fibronectin is reported to play a role in ligament healing and the maintenance of soft tissues [32–34].

Previous *in vitro* studies have focused on investigating the most appropriate primary cells to support ligament regeneration. Different primary cell types including Achilles tendon, patellar tendon, medial collateral ligament, and ACL on 3D braided scaffolds were examined for the gene expression of type I collagen, type III collagen, and fibronectin—all markers of cell differentiation and matrix production [19]. ACL cells expressed higher levels of each of these genetic markers, suggesting that the scaffold supported the function of these cells. Rabbit ACL cells were seeded onto the PLLA matrix for further characterization of cellular responses such as cell adhesion and proliferation. Cells at earlier time points were observed to exhibit a spherical structure and slow cellular spreading, indicating less-than-optimal surface properties for cell adhesion. In a follow-up study aimed to achieve enhanced cellular attachment, the cell adhesion molecule fibronectin was absorbed onto the surfaces of the PLLA fibers used in the 3D braids [14]. Cell proliferation measurements and scanning electron microscopy (SEM) images confirmed the increase in cell growth with the addition of fibronectin to the scaffolds. Western blot analysis showed an increase in type I collagen production by cells seeded onto scaffolds with fibronectin, in comparison with scaffolds without fibronectin. Thus, modifying the biomaterial surface with cell adhesion molecules is a promising approach to improve cell attachment efficiency, cell proliferation, and long-term matrix production on the 3D braided matrix. Furthermore, recent promising evidence on the use of autologous stem cells in regenerative engineering has established its importance in developing a clinically enhanced strategy for ligament reconstruction.

In recent years, much emphasis in the field of regenerative engineering has been placed on utilizing point-of-care stem cell therapy. Point-of-care stem cell therapy is the process of extracting tissue from a patient, processing it to yield a higher fraction of stem cells, and then injecting the stem cells back into the patient in one setting. Bone marrow-derived mononuclear cells (BM-MNCs) represent an attractive cell source due to their ease of isolation from autologous sources, high capacity of self-replication, and ability to maintain their multipotent differentiation into both mesenchymal and non-mesenchymal tissue types [35–38]. The combination of BM-MNCs with regenerative-engineered scaffolds has been demonstrated to be a clinically practical approach for the regeneration of a variety of tissue systems [39–45]. For example, it has been shown that Healos (a type I collagen/hydroxyapatite matrix) soaked in bone marrow aspirate resulted in a similar regenerative capacity as autologous iliac crest bone in posterolateral lumbar spine fusions [45]. Therefore, an ACL regenerative engineering approach to enhance the regeneration of synthetic ligaments would be to utilize BM-MNCs in combination with a bioengineered and biodegradable 3D braided matrix.

The aim of this study was to modulate the surface properties of a pre-established 3D PLLA bioengineered ACL matrix to enhance its

ability to support cell adhesion and growth. To this end, PLLA braided microfiber matrices were given air plasma treatment and were coated with fibronectin through physical adsorption to enhance surface wettability and add cell adhesion epitopes, respectively. The efficiency of fibronectin adsorption was investigated based on the time of incubation and the fibronectin concentration. For cell adhesion, three different plasma treatment times and fibronectin concentrations were investigated. A clinically relevant cell source was utilized—namely, rabbit bone marrow-derived mesenchymal stem cells (R-BMMSCs)—in order to assess the effect of these surface modifications on cell adhesion and growth. It was hypothesized that plasma treatment and fibronectin adsorption on PLLA braided microfiber matrices would promote R-BMMSCs adhesion and proliferation, thereby developing an enhanced clinical strategy for ligament reconstruction.

2. Materials and methods

2.1. Materials

PLLA yarns (molecular weight = 120 000 Da; inherent viscosity = 1.2–1.6; 120 Denier per 30 filaments) were purchased from Biomedical Structures LLC (USA). Fibronectin from human plasma (catalog number (cat#) 33016015, Gibco™, Thermo Fisher Scientific Inc., USA), with a molecular weight of 440 000 Da, was obtained from Life Technologies Corporation (USA). R-BMMSCs containing 1×10^6 cells per vial (cat# RBXMX-01001) were obtained from Cyagen Biosciences Inc. (USA). CellTiter-Blue® was purchased from Promega Corporation (USA). Protein conjugating dye from the Alexa Fluor 488 kit was obtained from Life Technologies Corporation. Dulbecco's Minimum Essential Medium (DMEM; cat# 11995), penicillin–streptomycin (cat# 15070-063), fetal bovine serum (cat# 16000-044), phosphate-buffered saline (PBS; cat#10010), and 0.05% trypsin-ethylene diamine tetraacetic acid (EDTA; cat# 25300-054) were purchased from Life Technologies Corporation.

2.2. Fabrication of PLLA braided microfiber matrices

PLLA braided microfiber matrices were fabricated via a braiding technique. In this technique, 20 yarns were laced to produce yarn bundles. Three yarn bundles were then individually tied to a hinge pin. 3D braided matrices were made by sequentially moving the yarns across each other in an alternating fashion by hand. Once the braiding was completed, individual matrices (10 mm × 3 mm) were cut and their ends knotted using an electric gun. The matrices were sterilized by incubating them in a conical tube (15 mL) containing 70% ethanol, and were then air dried in a biological safety cabinet (NuAire, USA). The matrices were then exposed to ultraviolet (UV; wave length = 254 nm) for 30 min on both sides to complete the sterilization process.

2.3. Air plasma treatment

PLLA braided microfiber matrices were air plasma treated at about 0.2 Torr (1 Torr = 133.322 Pa) air pressure in a Harrick plasma cleaner at the medium power setting for varying exposure times (5, 10, and 15 min, respectively). The effect of surface treatment on hydrophilicity was observed by water contact angle (WCA). WCA measurements were conducted using an optical contact angle (OCA) goniometer (Future Digital Scientific Corp., USA) equipped with a high-speed camera. For WCA measurements, flat samples were made by placing each piece of yarn adjacent to each other. Samples measuring 1 cm × 5 cm were then cut from the yarn bundles, placed in the sample stage, and held by double-sided carbon tape. Deionized water was dispensed at a rate of 1.5 $\mu L \cdot s^{-1}$ from a 50 μL syringe through a metallic needle (0.18 mm). Upon contact, an image with the WCA was automatically captured by the instrument.

2.4. Fibronectin adsorption onto PLLA braided microfiber matrices

Fibronectin adsorption studies were conducted to investigate the effect of fibronectin concentration and incubation time on fibronectin coverage onto PLLA braided microfiber matrices. Alexa Fluor 488 dye was conjugated with fibronectin to evaluate the distribution of fibronectin onto the matrices. Alexa Fluor 488-fibronectin conjugation was carried out following the manufacturer's protocol. To summarize, fibronectin stock solution (1 $mg \cdot mL^{-1}$) was warmed to room temperature and mixed with the dye in an amber vial. The protein dye was eluted through the manufacturer's custom-made liquid chromatogram column. The eluted protein–dye conjugate was homogenized and quantitated using an UV spectrophotometer. The labeled fibronectin molarity (molar concentration, M) was then calculated following Beer–Lambert's law, using the equation:

$$M = \frac{[A_{280} - (A_{494} \times 0.11)] \times \text{dilution factor}}{\varepsilon}$$

where A_{280} and A_{494} are the absorption at 280 and 494 nm, respectively, and ε is the molar attenuation coefficient (ε = 677 800 $L \cdot mol^{-1} \cdot cm^{-1}$). The dilution factor was 1, and a correction factor of 0.11 was applied to account for absorption of the dye at 280 nm. A series of solutions (10, 25, and 50 $\mu g \cdot mL^{-1}$) was made from the labeled fibronectin stock solution, and matrices were incubated in a small (2 mL) vial containing fibronectin solutions (10, 25, and 50 $\mu g \cdot mL^{-1}$) for various incubation times (30, 60, and 120 min) at 25 °C with constant agitation. After incubation, the loosely bound fibronectin was removed by washing the matrices three times in PBS. Bound fibronectin content was determined through an indirect method by measuring the fibronectin concentration in the solution before and after incubation in a microplate reader (Synergy™ HT, BioTek Instruments, Inc., USA).

2.5. Cell culture

R-BMMSCs were cultured in a T-75 flask with DMEM supplemented with MSC qualified 10% fetal bovine serum, 100 units (one unit represents the specific activity in 0.6 μg of sodium penicillin) of penicillin per milliliter ($U \cdot mL^{-1}$), and 50 $\mu g \cdot mL^{-1}$ streptomycin. Cells were incubated in an incubator at 37 °C with 95% humidified air and 5% carbon dioxide (CO_2). The medium was changed every two days and passaged every fourth day. For cell seeding onto matrices, the matrices were placed in a cyto-one 24 well tissue culture plate at a seeding density of 10^5 cells per matrix, and passage numbers 4 through 6 were utilized. The response of the R-BMMSCs on ① PLLA braided microfiber matrices, ② PLLA braided microfiber matrices + fibronectin, ③ PLLA braided microfiber matrices + air plasma treatment, and ④ air plasma treatment and fibronectin-adsorbed matrices were examined. Cultures were maintained for up to 21 d with the media being changed every other day.

2.6. Cell adhesion and proliferation

The adhesion and growth of R-BMMSCs on PLLA braided microfiber matrices were examined with respect to culture time, plasma treatment, and fibronectin adsorption. Cell adhesion was monitored using laser confocal microscopy and SEM. To determine cell adhesion at each time point (2, 8, and 24 h), samples were harvested and washed with PBS to remove non-adherent cells.

According to the manufacturer's protocol, the adhered cells were stained for cytoskeleton and nuclei using filamentous actin (F-actin) and propidium iodide, respectively. To summarize, the staining process was as follows: The cells were thoroughly rinsed with PBS and were fixed in 4% formalin for 20 min. Next, the cells were permeabilized for 5 min with 0.1 % Triton X-100 (in PBS). After further washing with PBS, 50 μL of F-actin staining (fluorescein isothiocyanate (FITC)-conjugated phalloidin) solution was added. Finally, nuclei were stained by propidium iodide and incubated for 20 min. The staining solutions were then removed, and the cells were imaged through a Zeiss (Germany) laser confocal microscope 510 Meta mounted on an Axiovert 200 M.

In addition, cell morphology on the PLLA braided microfiber matrices was examined via SEM. For SEM measurements, the cells were fixed for 1 h in 2.5% glutaraldehyde buffer. The fixed cells were then dehydrated using a graded series of ethanol solutions (30%, 50%, and 70% ethanol at 4 °C for 20 min; 90%, 95%, and 100% at room temperature for 20 min, followed by incubating the fixed cells in 100% ethanol overnight). SEM experiments were performed using JSM 6335F (JEOL Ltd., Japan) with an energy-dispersive X-ray spectroscopy attachment (Oxford, UK) at an acceleration voltage of 5 kV. Before SEM, samples (~0.5 cm diameter) were cut and placed onto a metallic stub by a double-sided carbon tape and coated with gold using a Polaron E5100 coating unit for about 45 s to yield a 10 nm coating.

The proliferation of R-BMMSCs on PLLA braided microfiber matrices was monitored using a CellTiter-Blue Cell Viability Assay (Promega Corporation, USA), following the manufacturer's instructions. The cells were rinsed thoroughly with PBS and incubated with 10% dye solution in the media for 2 h; 100 μL of the mixture was then transferred into 96 well plates, and the fluorescence was read at excitation/emission wavelengths of 530/590 nm, using a Synergy™ HT microplate reader (BioTek Instruments, Inc., USA). The cell numbers on the matrices were estimated based on a standard curve with known cell numbers.

2.7. Statistical analysis

Cell adhesion and proliferation data were analyzed using GraphPad Prism 7.00. Each time point was analyzed with one-way analysis of variance (ANOVA) with Tukey's *post hoc* analysis. All data was plotted as mean ± standard deviation. $p < 0.05$ was considered as significant. $n = 3$ was used for the cell adhesion kinetics studies. All other studies were $n = 4$.

3. Results and discussion

3.1. Optimization of fibronectin adsorption

Fig. 1 illustrates a schematic of the experimental groups along with a representative SEM image of the PLLA braided microfiber matrices. The PLLA braided microfiber matrices were either treated with ① fibronectin, ② air plasma treatment, or ③ air plasma treatment and fibronectin-adsorbed matrices. First, fibronectin adsorption onto the PLLA braided microfiber matrix was assessed by varying both the concentration and incubation time of the fibronectin solution. Through the use of fluorescently tagged fibronectin, it was observed that fibronectin adsorption on the PLLA braided microfiber matrix could be modulated by the concentration of fibronectin utilized during incubation (Figs. 2(a)–(d)). We next sought to determine the effects of incubation time on fibronectin adsorption. It was found that a 120 min incubation time in a 25 $\mu g \cdot mL^{-1}$ fibronectin solution resulted in a significant increase in the fibronectin adsorbed onto the PLLA braided microfiber matrix (Fig. 2(e)) and significantly enhanced the fibronectin adsorption efficiency (Fig. 2(f)). Fibronectin adsorption began to plateau at 2 h, and a linear trend was not conserved from the 30 to 60 to 120 min time points. Depending on the fibronectin concentration used and the substrate type, most studies have indicated that optimal incubation times can be up to 4 h [46,47]. Our finding that fibronectin binding plateaus at approximately the 120 min time point (Fig. 2(e)) is within the range of a study on PLLA films that showed rapid fibronectin adsorption up to the 60 min point, after which the adsorption plateaued [48]. The higher surface area of the PLLA braided microfiber matrix may account for the increased time for the saturation of fibronectin binding.

Fig. 2(g) shows that the fibronectin concentration has a direct relationship with fibronectin adsorption to the PLLA braided microfiber matrices. Incubating the matrices in 50 $\mu g \cdot mL^{-1}$ of

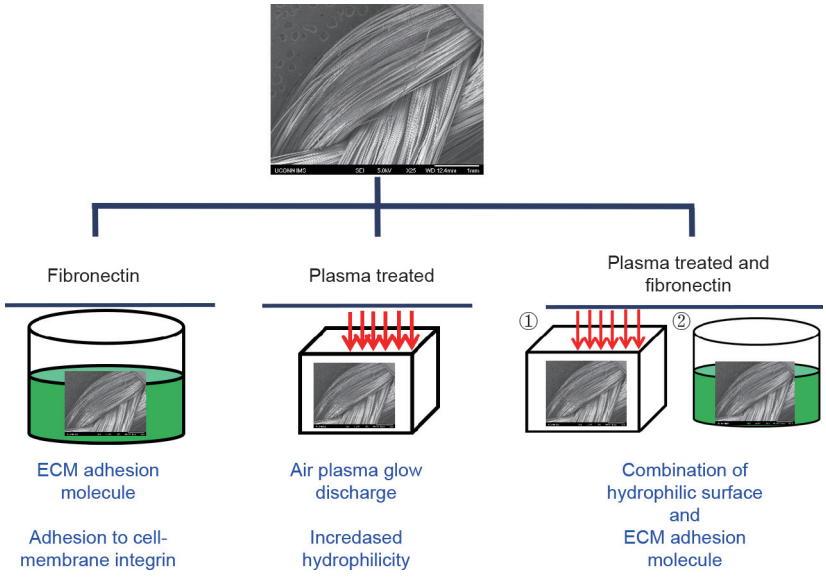

Fig. 1. Schematic of surface-modification techniques: (top) representative SEM image of braided PLLA biomimetic matrix; (bottom left) incubation of PLLA biomimetic matrix in a fibronectin solution of varying concentration; (bottom middle) exposure to air plasma glow discharge; (bottom right) exposing the PLLA biomimetic matrix to air plasma glow discharge followed by incubation in a fibronectin solution.

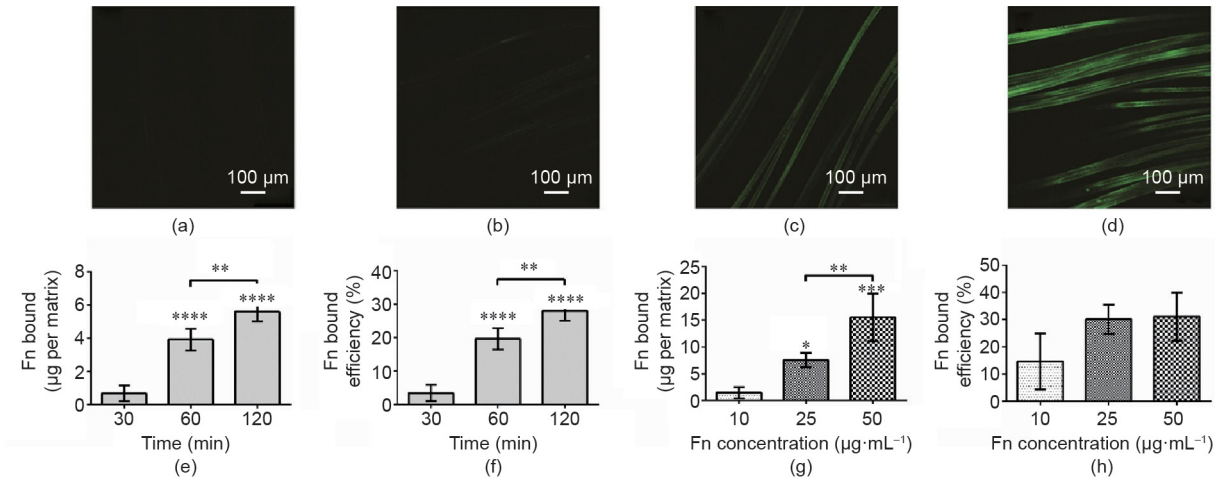

Fig. 2. Effect of surface treatment of fibronectin (Fn) absorption and surface properties of the PLLA braided microfiber matrix. (a–d) Fn–Alexa Fluor 488 absorption on biomimetic scaffold after 120 min incubation in PBS solution with (a) no Fn, (b) 0.1 μg·mL^{-1} Fn, (c) 1 μg·mL^{-1} Fn, and (d) 10 μg·mL^{-1} Fn. (e) Modulation of Fn binding (25 μg·mL^{-1} in PBS) on a PLLA braided microfiber matrix with time. (f) Efficiency of Fn binding as depicted in (e). (g) Modulation of Fn absorption after 120 min incubation in varying concentrations. (h) Efficiency of Fn binding as depicted in (g). *: $p < 0.05$; **: $p < 0.01$; ***: $p < 0.001$.

fibronectin for 120 min resulted in a significant increase in fibronectin adsorption, compared with fibronectin concentrations of 10 and 25 μg·mL^{-1}. However, the efficiency of fibronectin adsorption to the PLLA braided microfiber matrices incubated in 50 μg·mL^{-1} solution was not significantly different from the efficiency of adsorption onto matrices incubated in 25 μg·mL^{-1} fibronectin solution (Fig. 2(h)). Since the fibronectin binding efficiency between solutions containing fibronectin (25 and 50 μg·mL^{-1}) was statistically similar, matrices treated with 25 μg·mL^{-1} were chosen for further experiments. The importance of understanding fibronectin adsorption efficiency was based on the potential commercialization of the process, in which increased efficiency might reduce processing costs.

Our study demonstrated a fibronectin adsorption maximum at 50 μg·mL^{-1}, and showed that the binding efficiency plateaus at 25 μg·mL^{-1}, indicating that the saturation of fibronectin density occurred on the biomaterial surface between 10 and 25 μg·mL^{-1} (Fig. 2(h)). The plateau in the fibronectin binding efficiency indicated saturation of the fibronectin monolayer with an increase in fibronectin concentration, thereby preventing further adsorption of the fibronectin. This finding is consistent with previous observations on other polymer fibronectin systems [31]. In addition to protein concentration, incubation times have been found to have a significant role in predetermining the rate of fibronectin adsorption.

3.2. Effects of surface modifications on R-BMMSCs adhesion

R-BMMSCs adhesion due to surface modification was quantified by the cell number attached to the PLLA braided microfiber matrices. In addition, cell morphology was observed by immunofluorescence and SEM. Adsorption of fibronectin was found to promote cell adhesion at the 24 h time point, with a significant increase in the cell number exhibited on the PLLA braided microfiber matrices incubated in 10 and 25 μg·mL^{-1} fibronectin solution (Fig. 3(a)). A temporal cell adhesion experiment was subsequently conducted to gain an understanding of the cell adhesion kinetics. Cell adhesion was characterized over 24 h (time points of 0.5, 2, 4, 8, and 24 h) with a fibronectin coating concentration of 25 μg·mL^{-1}. The presence of fibronectin coating on the matrices significantly increased the cell adhesion, beginning as early as 0.5 h after cell seeding (Fig. 3(b), $p \leq 0.0001$), and this trend continued as the incubation time increased. The increase in cell adhesion after only 0.5 h of cell seeding is clinically relevant, since ACL reconstruction surgeries generally take 1–2 h.

Air plasma treatment of the PLLA braided microfiber matrices was found to decrease the WCA (Fig. S1 in Appendix A.) and enhance R-BMMSCs adhesion. The plasma-treated PLLA braided microfiber matrices demonstrated significantly higher cell adhesion 24 h post cell seeding, and the addition of fibronectin onto the air-plasma-treated matrices was found to enhance R-BMMSCs adhesion further (Fig. 3(c)). However, air plasma treatment for > 5 min resulted in a trend toward less cell adhesion. Air plasma treatment promotes cell adhesion by increasing the hydrophilicity, and the hydrophilicity is enhanced either by increasing the surface roughness [49] or through the addition of functional groups such as carbonyl groups [50]. An overly hydrophilic surface can negatively affect cell adhesion; a WCA between 60° and 80° has been cited as optimal for cell adhesion, but may vary based on the biomaterial [50]. In this study, it was found that the PLLA WCA was 79°; it decreased to 49° with 5 min of air plasma treatment, and was further reduced to 44° at 10 min, indicating a potential cause for the decreased cell adhesion. Given these results, air plasma treatment for 5 min was chosen for subsequent long-term proliferation experiments.

Fig. 3(e) demonstrates the morphology of the cells seeded on ① PLLA braided microfiber matrices, ② PLLA braided microfiber matrices + fibronectin, ③ PLLA braided microfiber matrices + air plasma treatment, and ④ air plasma treatment and fibronectin-adsorbed matrices, observed by means of immunostaining experiments. At 2 h post seeding, the R-BMMSCs had a spherical cellular morphology on the untreated PLLA braided microfiber matrices. In contrast, at the same time point, the cells on the surface-modified groups had elongated surface morphology. At both 8 h and 24 h, the R-BMMSCs on the PLLA braided microfiber matrices tended to form elongated cellular morphology. However, by this time point, the R-BMMSCs under both the air plasma treatment and the combined air plasma treatment with fibronectin-coated matrices showed longer spindle-like morphology with a larger surface area. These observations were further corroborated by SEM images (Fig. 3(f)) that showed fewer attached cells on the PLLA braided microfiber matrices at the 2 h time point. The trend continued at later time points, when fewer adhered cells were observed on the PLLA braided microfiber matrices, while those that

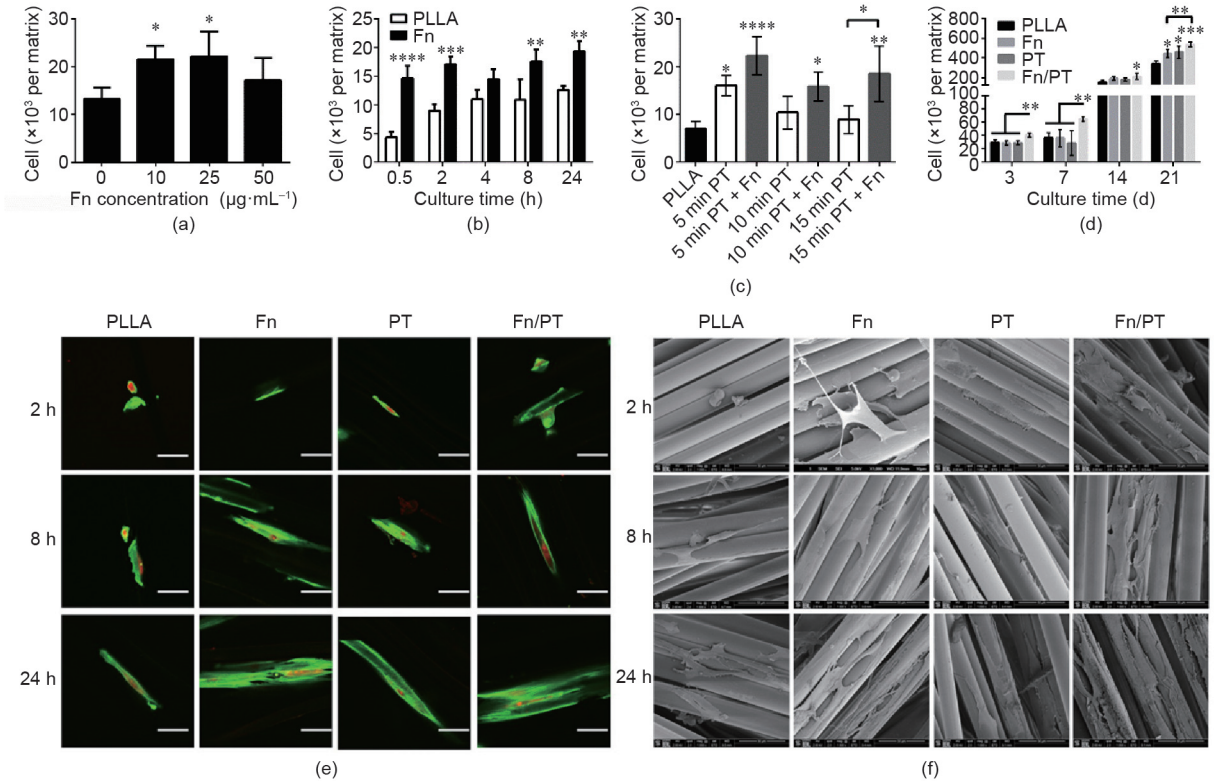

Fig. 3. Effect of surface treatment on R-BMMSCs adhesion. (a) R-BMMSCs adhesion as a function of Fn coating conditions 24 h post cell seeding. (b) Adhesion kinetics of R-BMMSCs on untreated PLLA ACL matrix and PLLA ACL matrix with Fn. (c) R-BMMSCs adhesion due to plasma treatment and the addition of Fn. (d) Long-term cell viability assessment of optimized surface modification experimental groups (Fn: incubation in 20 μg·mL^{-1} fibronectin solution; plasma treatment (PT): 5 min exposure to air plasma glow discharge; Fn/PT: exposure to air plasma glow discharge followed by incubation in Fn solution). (e, f) R-BMMSCs adhesion as a function of time and surface treatment: (e) immunostaining and (f) SEM. All error bars represent standard deviation. *: $p < 0.05$; **: $p < 0.01$; ***: $p < 0.001$; ****: $p < 0.0001$.

were air plasma treated or were air plasma treated with fibronectin coating showed more cells adhered onto the matrix. A similar trend in cell adhesion kinetics for human bone marrow stem cells has been previously reported: Deligianni et al. [51] demonstrated that human bone marrow stem cells seeded on hydroxyapatite matrices had round morphology 2 h post cell seeding, and that the cells began to elongate at 18 h. It has also been reported that the inclusion of fibronectin onto glass slides significantly decreases the time for fibroblasts to adhere, from 316.7 to 18.92 min, and significantly increases the number of cellular extensions as early as 5 h post seeding [52]. Collectively, these findings indicate that fibronectin adsorption and air plasma treatment on PLLA braided microfiber matrices are valid approaches to enhance cell adhesion.

3.3. Long-term R-BMMSCs viability and ECM deposition

Fig. 3(d) shows the long-term cell growth of R-BMMSCs on ① PLLA braided microfiber matrices, ② PLLA braided microfiber matrices + fibronectin, ③ PLLA braided microfiber matrices + air plasma treatment, and ④ air plasma treatment and fibronectin-adsorbed matrices. At day 3 and day 7, the air-plasma-treated and fibronectin-adsorbed matrices demonstrated significantly more cells than the control and other surface-modified groups. One potential explanation for this difference could lie in the surface chemistry of PLLA. Keselowsky et al. [53] demonstrated that surface chemistry modulates fibronectin conformation and leads to differential cell adhesion. At day 14, the plasma-treated and fibronectin-adsorbed matrices demonstrated a significant increase in R-BMMSCs number, compared with the unmodified PLLA braided microfiber matrices, but no significance was noted between the air-plasma-treated or fibronectin-adsorbed groups. Finally, at day 21, the synergistic effects of air plasma treatment and fibronectin outperformed both the untreated matrices and the fibronectin-adsorbed matrices, yet no difference was seen between the air-plasma-treated matrices and the air-plasma-treated with fibronectin-adsorbed matrices. Collectively, the evaluation of cell growth to 21 d demonstrates that the surface modifications are not cytotoxic.

R-BMMSCs distribution on various matrices was visualized by both SEM and immunostaining to further reveal the cellular compatibility of matrices after surface modification. Cell coverage on the surface-modified groups was observed to be more uniform than on the unmodified PLLA braided microfiber matrices after 21 d in culture (Fig. 4, upper panel). Enhanced cell coverage on the surface-modified groups was corroborated by representative immunostaining images, which demonstrated greater cell number and coverage by nuclei and cytoskeleton staining (Fig. 4, lower panel).

We also observed that the microfibers in the PLLA braided microfiber matrices contributed to anisotropic cell alignment. Studies have demonstrated that sub-micron aligned fibers demonstrate anisotropic cell alignment, yet this is also achieved on PLLA microfibers that are 15–20 μm in diameter [54,55]. As shown in Figs. 5(a) and (b), the R-BMMSCs growing along the fibers had elongated cell morphology after 21 d of culture. In addition, we found that the PLLA braided microfiber matrices modified by air plasma treatment and fibronectin adsorption were confluent with the aligned R-BMMSCs (Figs. 5(d) and (e)). Moreover, the synergistic effect of air plasma treatment and fibronectin-adsorbed matrices resulted in nanofibrous ECM deposition at day 21 (Fig. 5(f)). Nanofibrous ECM deposition suggested that the combined surface treatment used here may serve well to stimulate new tissue matrix

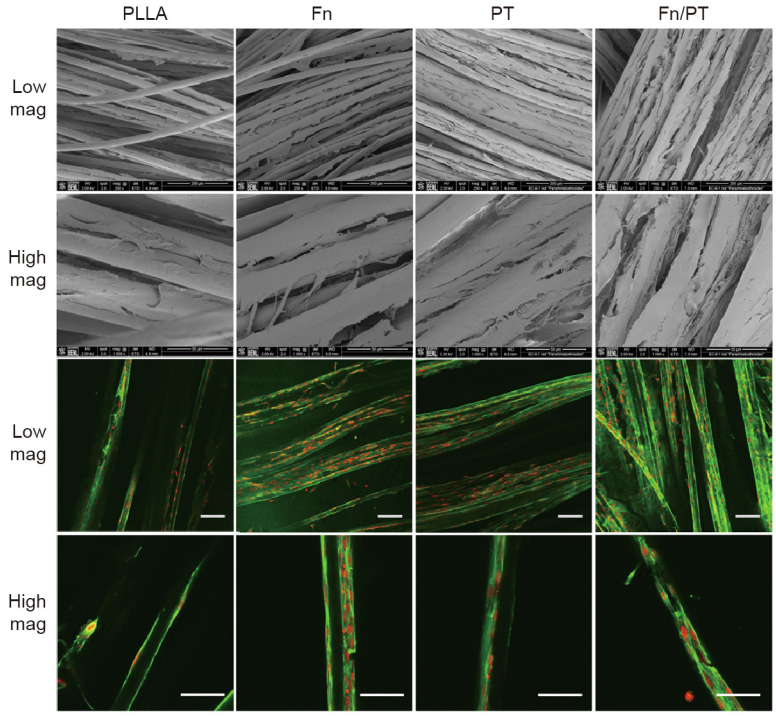

Fig. 4. R-BMMSCs growth and distribution of various matrices with different treatments. (Upper panel) SEM micrograph of R-BMMSCs growing on matrices shows more uniform cell distribution on Fn, PT, and Fn/PT groups compared with the PLLA control group at day 21. (Lower panel) immunostaining of R-BMMSCs growing on matrices: green: actin; red: nucleus (low magnification (mag) scale bar: 100 μm; high mag: 50 μm).

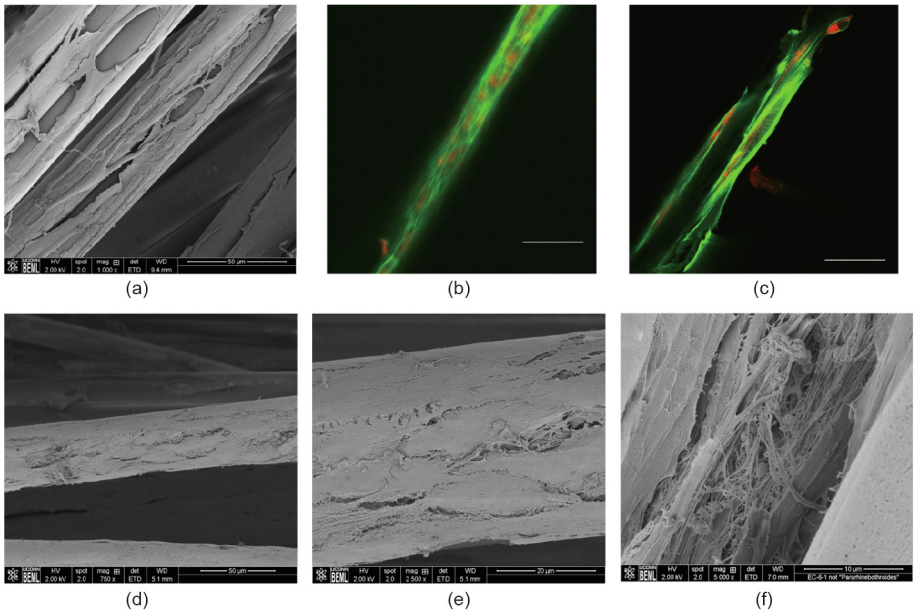

Fig. 5. R-BMMSCs alignment and ECM deposition on Fn/PT-treated matrices at day 21. (a) Elongated R-BMMSCs on Fn/PT matrices. (b, c) Immunostaining of R-BMMSCs cytoskeleton on Fn/PT. (d, e) SEM micrograph of PLLA microfiber (on Fn/PT group) covered with a layer of R-BMMSCs after 21 d of culture. (f) Nanofibrous ECM deposited on PLLA microfiber by R-BMMSCs.

formation in an aligned fashion that will contribute to the mechanical strength of implanted PLLA braided microfiber matrices. As the matrix degrades *in vivo*, the mechanical loads of the ACL will transfer to the deposited ECM. Thus, highly aligned ECM is important in maximizing the tensile strength of the graft over time.

In this study, we demonstrate that modifying the surface of PLLA braided microfiber matrices with air plasma treatment and fibronectin can significantly enhance cell adhesion as early as 30 min post cell seeding. In addition, we demonstrate that the morphology of the seeded R-BMMSCs elongates earlier on modified surfaces. Early cell adhesion and spreading is desired for the PLLA braided microfiber matrix for the potential application of point-of-care stem cell therapy during orthopedic applications. The application of bone marrow aspirate concentrate in ACL reconstruction has received recent attention [56]; thus, enhancing the cell adhesion within the operative time frame would be

advantageous to promote cell retention on the matrix during implantation. Although it is not investigated here, cell spreading is known to correlate with cell adhesion strength [57], and sufficient cell adhesion strength is necessary to withstand the forces exerted on the matrix during implantation. Future studies may probe into the effect of surface modification on cell adhesion strength with the PLLA braided microfiber matrix, and may investigate the *in vivo* response.

4. Conclusions

PLLA braided microfiber matrices may serve as a viable alternative to the currently used autografts and allografts for ACL reconstruction. The advantage of a PLLA braided microfiber matrix is that it offers consistent material properties, as opposed to patient-to-patient tissue variability. Surface modification of PLLA braided microfiber matrices with air plasma treatment and fibronectin adsorption significantly enhanced cell adhesion and growth on the matrix. The enhanced cellular adhesion properties of the PLLA braided microfiber matrix may be attractive for point-of-care therapies such as the application of bone marrow aspirate concentrate, leading to greater cell adhesion before implantation of the matrix. The enhanced cellular adhesion and proliferation of surface-modified PLLA braided microfiber matrices may lead to enhanced and accelerated ACL regeneration *in vivo*.

Acknowledgements

This research was supported by funding from the Raymond and Beverly Sackler Center for Biomedical, Biological, Physical and Engineering Sciences (NIH R01AR063698, NIH R01AR063698-02S1, and NIH DP1 AR068147). The authors wish to disclose that Cato T. Laurencin and Lakshmi S. Nair have ownership and company interests in Biorez, Incorporated.

Authors' contribution

Xiaohua Yu performed experiments, performed data analysis, and prepared figures. Paulos Y. Mengsteab performed experiments, performed data analysis, prepared figures, and wrote the manuscript. Ganesh Narayanan assisted in manuscript composition. Lakshmi S. Nair and Cato T. Laurencin oversaw experiments and assisted in manuscript composition.

Compliance with ethics guidelines

Dr. Cato T. Laurencin has the following competing financial interests: Biorez, Globus, HOT, HOT Bone, Kuros Bioscience, NPD & Cobb (W. Montague) NMA Health Institute. Dr. Lakshmi S. Nair has the following competing financial interests: Biorez. Xiaohua Yu, Paulos Y. Mengsteab, Ganesh Narayanan, Lakshmi S. Nair, and Cato T. Laurencin have no other conflict of interest (non-financial) to disclose.

Appendix A. Supplementary data

Supplementary data to this article can be found online at https://doi.org/10.1016/j.eng.2020.02.010.

References

[1] Mather RC, Hettrich CM, Dunn WR, Cole BJ, Bach BR Jr, Huston LJ, et al. Cost-effectiveness analysis of early reconstruction versus rehabilitation and delayed reconstruction for anterior cruciate ligament tears. Am J Sports Med 2014;42(7):1583–91.
[2] Biau DJ, Tournoux C, Katsahian S, Schranz PJ, Nizard RS. Bone-patellar tendon-bone autografts versus hamstring autografts for reconstruction of anterior cruciate ligament: meta-analysis. BMJ 2006;332(7548):995–1001.
[3] Predescu V, Georgeanu V, Prescura C, Stoian V, Cristea S. Anterior cruciate ligament reconstruction: soft tissue vs bone–tendon–bone. In: Proceedings of the 2nd Advanced Technologies for Enhanced Quality of Life; 2010 Jul 15–19; Iasi, Romania. New York: IEEE; 2010. p. 53–7.
[4] Magnussen RA, Carey JL, Spindler KP. Does autograft choice determine intermediate-term outcome of ACL reconstruction? Knee Surg Sports Traumatol Arthrosc 2011;19(3):462–72.
[5] Richmond JC, Manseau CJ, Patz R, McConville O. Anterior cruciate reconstruction using a Dacron ligament prosthesis. A long-term study. Am J Sports Med 1992;20(1):24–8.
[6] Moyen BJ, Jenny JY, Mandrino AH, Lerat JL. Comparison of reconstruction of the anterior cruciate ligament with and without a Kennedy ligament-augmentation device. A randomized, prospective study. J Bone Joint Surg Am 1992;74(9):1313–9.
[7] Freeman JW, Kwansa AL. Recent advancements in ligament tissue engineering: the use of various techniques and materials for ACL repair. Recent Pat Biomed Eng 2008;1(1):18–23.
[8] Legnani C, Ventura A, Terzaghi C, Borgo E, Albisetti W. Anterior cruciate ligament reconstruction with synthetic grafts. A review of literature. Int Orthop 2010;34(4):465–71.
[9] Olson EJ, Kang JD, Fu FH, Georgescu HI, Mason GC, Evans CH. The biochemical and histological effects of artificial ligament wear particles: *in vitro* and *in vivo* studies. Am J Sports Med 1988;16(6):558–70.
[10] Mengsteab PY, Nair LS, Laurencin CT. The past, present and future of ligament regenerative engineering. Regen Med 2016;11:871–81.
[11] Mengsteab PY, McKenna M, Cheng J, Sun Z, Laurencin CT. Regenerative strategies for the treatment of knee joint disabilities. Berlin: Springer International Publishing; 2017. p. 391–410.
[12] Cooper JA, Sahota JS, Gorum WJ, Carter J, Doty SB, Laurencinl CT. Biomimetic tissue-engineered anterior cruciate ligament replacement. Proc Nat Acad Sci USA 2007;104(9):3049–54.
[13] Mengsteab PY, Conroy P, Badon M, Otsuka T, Kan HM, Vella AT, et al. Evaluation of a bioengineered ACL matrix's osteointegration with BMP-2 supplementation. PLoS ONE 2020;15:1–18.
[14] Lu HH, Cooper JA, Manuel S, Freeman JW, Attawia MA, Ko FK, et al. Anterior cruciate ligament regeneration using braided biodegradable scaffolds: *in vitro* optimization studies. Biomaterials 2005;26:4805–16.
[15] Nair LS, Laurencin CT. Biodegradable polymers as biomaterials. Prog Polym Sci 2007;32:762–98.
[16] Laurencin CT, Freeman JW. Ligament tissue engineering: an evolutionary materials science approach. Biomaterials 2005;26:7530–6.
[17] Cooper JA, Lu HH, Ko FK, Freeman JW, Laurencin CT. Fiber-based tissue-engineered scaffold for ligament replacement: design considerations and *in vitro* evaluation. Biomaterials 2005;26:1523–32.
[18] Yahia L. Ligaments and ligamentoplasties. Berlin: Springer; 1997.
[19] Cooper JA, Bailey LO, Carter JN, Castiglioni CE, Kofron MD, Ko FK, et al. Evaluation of the anterior cruciate ligament, medial collateral ligament, achilles tendon and patellar tendon as cell sources for tissue-engineered ligament. Biomaterials 2006;27:2747–54.
[20] Stevens MM, George JH. Exploring and engineering the cell surface interface. Science 2005;310(80):1135–8.
[21] Hallab NJ, Bundy KJ, O'Connor K, Moses RL, Jacobs JJ. Evaluation of metallic and polymeric biomaterial surface energy and surface roughness characteristics for directed cell adhesion. Tissue Eng 2001;7:55–71.
[22] Hanson AD, Wall ME, Pourdeyhimi B, Loboa EG. Effects of oxygen plasma treatment on adipose-derived human mesenchymal stem cell adherence to poly(*L*-lactic acid) scaffolds. J Biomater Sci Polym Ed 2007;18(11):1387–400.
[23] Rosso F, Giordano A, Barbarisi M, Barbarisi A. From cell-ECM interactions to tissue engineering. J Cell Physiol 2004;199(2):174–80.
[24] Sahoo S, Cho-Hong JG, Siew-Lok T. Development of hybrid polymer scaffolds for potential applications in ligament and tendon tissue engineering. Biomed Mater 2007;2:169–73.
[25] Leiss M, Beckmann K, Girós A, Costell M, Fässler R. The role of integrin binding sites in fibronectin matrix assembly *in vivo*. Curr Opin Cell Biol 2008;20:502–7.
[26] Millard CJ, Ellis IR, Pickford AR, Schor AM, Schor SL, Campbell ID. The role of the fibronectin IGD motif in stimulating fibroblast migration. J Biol Chem 2007;282(49):35530–5.
[27] Hall BK, Miyake T. All for one and one for all: condensations and the initiation of skeletal development. Bioassays 2000;22(2):138–47.
[28] Sechler JL, Schwarzbauer JE. Control of cell cycle progression by fibronectin matrix architecture. J Biol Chem 1998;273:25533–6.
[29] Cheng X, Gurkan UA, Dehen CJ, Tate MP, Hillhouse HW, Simpsonet GJ, et al. An electrochemical fabrication process for the assembly of anisotropically oriented collagen bundles. Biomaterials 2008;29:3278–88.
[30] Bhati RS, Mukherjee DP, McCarthy KJ, Rogers SH, Smith DF, Shalaby SW. The growth of chondrocytes into a fibronectin-coated biodegradable scaffold. J Biomed Mater Res 2001;56:74–82.
[31] García AJ, Vega MD, Boettiger D. Modulation of cell proliferation and differentiation through substrate-dependent changes in fibronectin conformation. Mol Biol Cell 1999;10:785–98.
[32] Gelberman RH, Steinberg D, Amiel D, Akeson W. Fibroblast chemotaxis after tendon repair. J Hand Surg Am 1991;16:686–93.

[33] Neurath M. Expression of tenascin, laminin and fibronectin following traumatic rupture of the anterior cruciate ligament. Z Orthop Ihre Grenzgeb 1993;131(2):168–72.
[34] Amiel D, Foulk RA, Harwood FL, Akeson WH. Quantitative assessment by competitive ELISA of fibronectin (Fn) in tendons and ligaments. Matrix 1990;9:421–7.
[35] Caplan AI. Adult mesenchymal stem cells for tissue engineering versus regenerative medicine. J Cell Physiol 2007;213:341–7.
[36] Caterson EJ, Nesti LJ, Danielson KG, Tuan RS. Human marrow-derived mesenchymal progenitor cells. Mol Biotechnol 2002;20:245–56.
[37] Jiang Y, Jahagirdar BN, Reinhardt RE, Schwartz RE, Keene CD, Ortiz-Gonzalezet XR, et al. Pluripotency of mesenchymal stem cells derived from adult marrow. Nature 2002;418(6893):41–9.
[38] Jager M, Jelinek EM, Wess KM, Scharfstadt A, Jacobson M, Kevy SV, et al. Bone marrow concentrate: a novel strategy for bone defect treatment. Curr Stem Cell Res Ther 2009;4(1):34–43.
[39] Segers VFM, Lee RT. Stem-cell therapy for cardiac disease. Nature 2008;451:937–42.
[40] Gómez-Barrena E, Rosset P, Müller I, Giordano R, Bunu C, Layrolle P, et al. Bone regeneration: stem cell therapies and clinical studies in orthopaedics and traumatology. J Cell Mol Med 2011;15:1266–86.
[41] Jäger M, Herten M, Fochtmann U, Fischer J, Hernigou P, Zilkens C, et al. Bridging the gap: bone marrow aspiration concentrate reduces autologous bone grafting in osseous defects. J Orthop Res 2011;29:173–80.
[42] Roh JD, Nelson GN, Udelsman BV, Brennan MP, Lockhart B, Fong PM, et al. Centrifugal seeding increases seeding efficiency and cellular distribution of bone marrow stromal cells in porous biodegradable scaffolds. Tissue Eng 2007;13:2743–9.
[43] Hisatome T, Yasunaga Y, Yanada S, Tabata Y, Ikada Y, Ochi M. Neovascularization and bone regeneration by implantation of autologous bone marrow mononuclear cells. Biomaterials 2005;26(22):4550–6.
[44] Hibino N, Nalbandian A, Devine L, Martinez RS, McGillicuddy E, Yi T, et al. Comparison of human bone marrow mononuclear cell isolation methods for creating tissue-engineered vascular grafts: novel filter system versus traditional density centrifugation method. Tissue Eng Part C Methods 2011;17:993–8.
[45] Neen D, Noyes D, Shaw M, Gwilym S, Fairlie N, Birch N. Healos and bone marrow aspirate used for lumbar spine fusion. Spine 2006;31(18):E636–40.
[46] Hindié M, Degat MC, Gaudière F, Gallet O, Van Tassel PR, Pauthe E. Pre-osteoblasts on poly(*L*-lactic acid) and silicon oxide: Influence of fibronectin and albumin adsorption. Acta Biomater 2011;7(1):387–94.
[47] Xu H, Deshmukh R, Timmons R, Nguyen KT. Enhanced endothelialization on surface modified poly(*L*-lactic acid) substrates. Tissue Eng Part A 2011;17:865–76.
[48] Jiao Y, Zhou C, Li L. Protein adsorption on the poly(*L*-lactic acid) surface modified by chitosan and its derivatives. Chinese Sci Bull 2009;54 (18):3167–73.
[49] Teraoka F, Nakagawa M, Hara M. Surface modification of poly(*L*-lactide) by atmospheric pressure plasma treatment and cell response. Dent Mater J 2006;25:560–5.
[50] Nakagawa M, Teraoka F, Fujimoto S, Hamada Y, Kibayashi H, Takahashi J. Improvement of cell adhesion on poly(*L*-lactide) by atmospheric plasma treatment. J Biomed Mater Res 2006;77(1):112–8.
[51] Deligianni DD, Katsala ND, Koutsoukos PG, Missirlis YF. Effect of surface roughness of hydroxyapatite on human bone marrow cell adhesion, proliferation, differentiation and detachment strength. Biomaterials 2000;22:87–96.
[52] Schlie-Wolter S, Ngezahayo A, Chichkov BN. The selective role of ECM components on cell adhesion, morphology, proliferation and communication *in vitro*. Exp Cell Res 2013;319:1553–61.
[53] Keselowsky BG, Collard DM, García AJ. Surface chemistry modulates fibronectin conformation and directs integrin binding and specificity to control cell adhesion. J Biomed Mater Res 2003;66A(Pt A):247–59.
[54] Jeon H, Simon CG, Kim G. A mini-review: cell response to microscale, nanoscale, and hierarchical patterning of surface structure. J Biomed Mater Res Part B Appl Biomater 2014;102(7):1580–94.
[55] Bettinger CJ, Langer R, Borenstein JT. Engineering substrate topography at the micro- and nanoscale to control cell function. Angew Chem Int Ed 2009;48:5406–15.
[56] Figueroa D, Calvo R, Vaisman A, Arellano S, Figueroa F, Donoso R, et al. Arthroscopic intercondylar notch bone marrow aspiration during anterior cruciate ligament reconstruction. Arthrosc Tech 2019;8(12): e1437–41.
[57] Truskey GA, Proulx TL. Relationship between 3T3 cell spreading and the strength of adhesion on glass and silane surfaces. Biomaterials 1993;14 (4):243–54.